Na,K-ATPase α2 activity in mammalian skeletal muscle T-tubules is acutely stimulated by extracellular K+

Marino DiFranco,[1] Hesamedin Hakimjavadi,[2] Jerry B. Lingrel,[2] and Judith A. Heiny[2]

[1]Department of Physiology, David Geffen School of Medicine, University of California, Los Angeles, Los Angeles, CA 90095
[2]Department of Molecular and Cellular Physiology, University of Cincinnati College of Medicine, Cincinnati, OH 45267

The Na,K-ATPase α2 isoform is the predominant Na,K-ATPase in adult skeletal muscle and the sole Na,K-ATPase in the transverse tubules (T-tubules). In quiescent muscles, the α2 isozyme operates substantially below its maximal transport capacity. Unlike the α1 isoform, the α2 isoform is not required for maintaining resting ion gradients or the resting membrane potential, canonical roles of the Na,K-ATPase in most other cells. However, α2 activity is stimulated immediately upon the start of contraction and, in working muscles, its contribution is crucial to maintaining excitation and resisting fatigue. Here, we show that α2 activity is determined in part by the K+ concentration in the T-tubules, through its K+ substrate affinity. Apparent K+ affinity was determined from measurements of the $K_{1/2}$ for K+ activation of pump current in intact, voltage-clamped mouse flexor digitorum brevis muscle fibers. Pump current generated by the α2 Na,K-ATPase, Ip, was identified as the outward current activated by K+ and inhibited by micromolar ouabain. Ip was outward at all potentials studied (−90 to −30 mV) and increased with depolarization in the subthreshold range, −90 to −50 mV. The Q_{10} was 2.1 over the range of 22–37°C. The $K_{1/2,K}$ of Ip was 4.3 ± 0.3 mM at −90 mV and was relatively voltage independent. This K+ affinity is lower than that reported for other cell types but closely matches the dynamic range of extracellular K+ concentrations in the T-tubules. During muscle contraction, T-tubule luminal K+ increases in proportion to the frequency and duration of action potential firing. This $K_{1/2,K}$ predicts a low fractional occupancy of K+ substrate sites at the resting extracellular K+ concentration, with occupancy increasing in proportion to the frequency of membrane excitation. The stimulation of preexisting pumps by greater K+ site occupancy thus provides a rapid mechanism for increasing α2 activity in working muscles.

INTRODUCTION

The Na,K-ATPase is an essential enzyme in the plasma membrane of all animal cells. The Na,K-ATPase catalyzes the efflux of three Na+ and the influx of two K+ ions per molecule of ATP hydrolyzed, thereby maintaining the steep transmembrane concentration gradients for Na+ and K+ that play a vital role in many biological processes.

The functional enzyme is a heteromer composed of a primary catalytic α subunit, a glycosylated β subunit, and in most cells a regulatory FXYD subunit (Kaplan, 2002). Four α isoforms (α1–α4), three β isoforms (β1–β3), and seven FXYD isoforms (FXYD1–FXYD7; Sweadner, 1989; Geering, 2008) have been identified. The α, β, and FXYD subunits combine to form a range of isozymes that show tissue, cellular, and subcellular patterns of distribution (Crambert et al., 2000).

The Na+/K+ transport cycle comprises a sequence of conformational transitions in which alternating access of extracellular K+ and intracellular Na+ ions to substrate sites, coupled to ATP hydrolysis, drives energetically uphill transport. Inward facing sites in the dephosphorylated enzyme bind Na+ with high affinity; outward facing sites in the phosphorylated enzyme bind K+ with high affinity. The transport rate of the enzyme, up to a maximum that is limited by the conformational transitions, is modulated by multiple mechanisms that match enzyme activity to changing demands. A primary mechanism for the acute regulation of enzyme activity is the fractional occupancy of the substrate sites for Na+ and K+. Cation binding is extremely rapid and occurs in the millisecond time range (Froehlich and Fendler, 1991; Heyse et al., 1994). Consequently, changes in substrate site occupancy produce rapid changes in enzyme activity.

The major Na,K-ATPase α isoform in most cell types is the ubiquitously expressed α1 subunit. Its apparent affinity for K+ ($K_{1/2,K}$) is near 1 mM, and its apparent affinity for Na+ is in the range of 8–16 mM (Blanco and Mercer, 1998; Crambert et al., 2000; Berry et al., 2007). Therefore, at rest, under typical physiological concentrations of extracellular K+ (4–5 mM) and intracellular Na+ (10–12 mM), K+ site occupancy is near maximal, and acute regulation of turnover rate by substrate occupancy is determined mainly by changes in intracellular Na+.

Correspondence to Marino DiFranco: MDiFranco@mednet.ucla.edu; or Judith A. Heiny: heinyja@ucmail.uc.edu

Abbreviations used in this paper: FDB, flexor digitorum brevis; T-tubule, transverse tubule; TTX, tetrodotoxin.

Mammalian skeletal muscles, however, operate over a wider range of extracellular K$^+$ and intracellular Na$^+$ concentrations than most other cell types. Quiescent skeletal muscles live in a 4-mM extracellular K$^+$ and 10-mM intracellular Na$^+$ environment (Eltit et al., 2013), whereas contracting muscles gain Na$^+$ and lose K$^+$ during repetitive action potential activity (Sejersted and Sjøgaard, 2000). These changes are significant at physiological contraction rates. Intracellular Na$^+$ can increase up to threefold in rodent skeletal muscles undergoing electrical stimulation (Fong et al., 1986; Everts and Clausen, 1994; Clausen, 2013). Extracellular K$^+$ can reach 8–10 mM in the muscle interstitial spaces (Vyskočil et al., 1983; Juel, 1988; Radzyukevich et al., 2009), and tens of millimolar in the lumen of the transverse tubules (T-tubules; Almers, 1980; Wallinga et al., 1999; Sejersted and Sjøgaard, 2000; Shorten and Soboleva, 2007; Fraser et al., 2011; Clausen, 2013). The K$^+$ load in the T-tubules increases in direct proportion to the intensity and duration of action potential activity. During intense exercise, up to 30,000 action potentials may be generated at frequencies from 25 to 100 Hz (Burke et al., 1973; Hennig and Lømo, 1985; Green, 2004).

The excitation-related K$^+$ load in the T-tubules poses a particular challenge for working muscles. Mammalian T-tubules encompass >80% of the total cell membrane but enclose <3% of the fiber volume (Eisenberg and Kuda, 1975). As a result of great limitations posed by the size and tortuosity of the T-tubules, diffusion alone is not sufficient to remove the excitation-related K$^+$ load that, if not opposed, can impair excitation (Kirsch et al., 1977; Clausen, 2003a).

Rodent skeletal muscles express two isozymes of the Na,K-ATPase, α1 and α2 (Orlowski and Lingrel, 1988). The α2 isozymes comprise most of the Na,K-ATPase pumps, reaching up to 90% of total α-subunit content in fast-twitch muscles (Orlowski and Lingrel, 1988; He et al., 2001). The α1 isoform is localized to the surface sarcolemma (Williams et al., 2001) and provides up to 75% of the basal Na$^+$/K$^+$ transport needed to maintain resting ion gradients and the resting potential (Krivoi et al., 2003; Chibalin et al., 2012). The α2 isoform is the sole Na,K-ATPase isozyme in the T-tubules. Although assembled and inserted into the membrane, it operates significantly below its maximal transport capacity in quiescent muscles (Krivoi et al., 2003; Radzyukevich et al., 2004; Chibalin et al., 2012). The α2 isoform does not set resting ion gradients (He et al., 2001) or the resting potential (Radzyukevich et al., 2004, 2013), the canonical roles of the Na,K-ATPase in most other cell types. However, α2 isozyme activity is rapidly increased upon the start of muscle excitation, and its contribution in working muscles is absolutely required to maintain contraction and oppose fatigue (Radzyukevich et al., 2013).

The mechanisms that acutely increase Na,K-ATPase activity in working skeletal muscles are not completely known. It is widely assumed, based on measurements in other cells and recombinant systems, that the rapid, excitation-related increases in Na,K-ATPase activity are determined primarily by increases in intracellular Na$^+$ (Semb and Sejersted,1996; Therien and Blostein, 2000; Clausen, 2013). However, the affinities of the separate isoforms for K$^+$ have not been determined in skeletal muscle.

This study tests the hypothesis that the apparent K$^+$ affinity of the α2 isoform, $K_{1/2,K}$, may be more closely matched to the K$^+$ concentrations that exist in the T-tubules during muscle excitation. A K$^+$ affinity in this range would allow the α2 isoform to respond dynamically to increases in extracellular K$^+$, under control of membrane excitation. We determined the $K_{1/2,K}$ for activation of α2 by extracellular K$^+$ from measurements of Na,K-ATPase pump currents in isolated mouse flexor digitorum brevis (FDB) muscle fibers voltage clamped with a two-microelectrode method. The contributions of the α1 and α2 Na,K-ATPase isoforms to total pump current were identified using low concentrations of ouabain to inhibit predominantly α2 pumps, and by comparing results using wild-type mice and skα2$^{-/-}$ mice. Wild-type mice express both isoforms with α2 predominating; skα2$^{-/-}$ mice have a targeted knockout of the α2 isoform and express only α1 in the skeletal muscles (Radzyukevich et al., 2013).

MATERIALS AND METHODS

Animals
Adult wild-type male mice (C57BL/6; The Jackson Laboratory) or genetically altered mice, skα2$^{-/-}$ (Radzyukevich et al., 2013), of 2–4 mo of age were used as a source of tissue. All procedures involving mice were performed in accordance with guidelines established by the Office of Animal Research Oversight of the University of California, Los Angeles, and the Institutional Animal Care and Use Committee of the University of Cincinnati. Tissue was removed from euthanized animals. Euthanasia was performed using deep anesthesia followed by cervical dislocation.

Single fiber preparation
Measurements were performed on single, isolated FDB fibers. The FDB muscle is a mixed, glycolytic muscle with a fast contractile phenotype (Edman, 2005). The FDB muscles of both feet were surgically removed and enzymatically dissociated to obtain single fibers, as described previously (Woods et al., 2004). In brief, muscles were pinned at the tendons to a Sylgard-coated dish and incubated with type 2 collagenase (1,000 U/ml dissolved in standard Tyrode's solution; Worthington Biochemical Corporation) for 35 min at 36°C, under mild agitation. The muscles were passed in and out of fire-polished Pasteur pipettes of progressively smaller diameters to obtain single fibers. Dissociated fibers were washed four to five times with a collagenase-free Tyrode's buffer and transferred to the experimental chamber. The wash promoted tight attachment of single fibers to the glass bottom of the experimental chamber. The preparation was maintained at room temperature in a covered Petri dish to avoid evaporation. Approximately 40–50 fibers from each batch were transferred, and selected fibers were used for recordings within the next 6–8 h. The criteria used to select fibers for recording

were: (a) a continuous smooth surface devoid of kinks; (b) sharply delineated striations; (c) the ability to withstand a flux of ∼1 ml/min from a 1.5-mm tubing without detaching from the coverslip; (d) upon impalement in Tyrode's buffer, the ability to polarize to −90 mV using <15 nA or <16 µA/cm²–injected current; (e) hyperpolarization of 30–40 mV after the change to 4K-EXT solution (see below), associated with a reduction in holding current at −90 mV to <7.8 µA/cm².

The experimental chamber consisted of a Petri dish with a perforated bottom (100-mm diameter) to which an untreated coverslip (no. 1) was attached with Sylgard (Corning) to form a well of ∼300 µl volume. The chamber was placed on the stage of an inverted microscope (IX71; Olympus). An image of each fiber was obtained at 10× at the start and end of each experiment and used to compute the outer surface area and average diameter of each fiber using a custom algorithm. The algorithm divides the fiber into 2-µm-long transverse segments. The outer surface area of each segment is obtained from that diameter assuming a cylindrical geometry, and the surface area of all segments is integrated over the fiber length to obtain total fiber surface area. The reported fiber diameter is the mean of the diameters of all segments, and fiber length is the sum of all segment lengths. The fibers used for recording had diameters of 42–65 µm (median: 51 µm; n = 73) and lengths of 420–640 µm (median 560 µm). Mean cylindrical fiber surface area was $0.94 \times 10^{-3} \pm 0.03 \times 10^{-3}$ cm², and mean fiber capacitance was 5.13 ± 0.12 µF/cm² of cylindrical surface area.

Experimental solutions

Before recording pump currents, muscles and dissociated fibers were maintained in a standard Tyrode's solution containing (mM): 150 NaCl, 4 KCl, 2 CaCl₂, 1 MgCl₂, 10 glucose, and 10 MOPS, pH 7.4. The extracellular solutions used to measure pump current, 0K- to 40K-EXT, contained: 0–40 mM KCl, 114–154 mM NaCl, 2 mM CaCl₂, 1 mM MgCl₂, 10 mM glucose, 10 mM MOPS, 200 µM 9-anthracene carboxylic acid (9-ACA), 20 µM nifedipine, 200 nM tetrodotoxin (TTX), and 4 mM Ba²⁺, pH 7.4. The indicated K⁺ and Na⁺ concentrations were achieved by mixing two solutions containing either 40 mM KCl and 114 mM NaCl or 0 mM KCl and 154 mM NaCl, while keeping constant the concentration of all other components. 9-ACA, nifedipine, TTX, and Ba²⁺ were included to block chloride (ClC1), calcium (Cav2.1), sodium (Nav4.1), and inward rectifier (Kir2.1, Kir2.2) channels. TTX and nifedipine prevented voltage-dependent Na⁺ and Ca²⁺ entry in experiments in which the membrane was depolarized. Stock solutions for 9ACA (500 mM) and nifedipine (50 mM) were prepared in DMSO, with final DMSO concentration in the working solutions kept <0.1%. 10 µM ouabain added to the extracellular solution was used to block the α2 isoform of the Na,K-ATPase. Stocks for ouabain (10 mM) and BaCl₂ (2 M) were prepared in aqueous solutions. The intracellular pipette solution contained (mM): 138 KOH, 10 KCl, 110 aspartic acid, 30 NaOH, 5 ATP-Na₂, 5 creatine phosphate-Na₂, 5 reduced glutathione, 5 MgCl₂, 1 or 30 EGTA, 0.5 or 15 CaCl₂, and 20 MOPS, pH 7.4. The use of 1 mM EGTA/ 0.5 mM Ca²⁺ or 30 mM EGTA/15 mM Ca²⁺ maintained intracellular free Ca²⁺ at 60–80 nM, near muscle resting levels, and prevented large changes in intracellular Ca²⁺ upon electrode impalement or depolarization. A low intracellular Ca²⁺ concentration also prevents outward Ca²⁺ transport from forward sodium–calcium exchange. The presence of saturating ATP and ATP-regenerating substrates maintains a high ATP to ADP/AMP ratio and favors forward pump cycling. Millimolar concentrations of ATP also favor the closed state of the inward rectifier K⁺ channel. All solutions had 300 ± 10 mOsmol/kg H₂O.

The chamber was continuously perfused with extracellular solution using gravity-fed syringes connected to inline valves and continuous aspiration from the liquid surface. Valve ports were selected manually, and complete exchange of the bath solution

was reached in <3 s (range of 2–5 s). Bath temperature was maintained using an inline temperature controller (Harvard Apparatus) and bath thermistor, placed ∼2 mm from the fiber under study.

Electrophysiology

Single FDB fibers were voltage clamped with a two-microelectrode method and amplifier (Dagan Corporation), essentially as described previously (Woods et al., 2004; DiFranco et al., 2005, 2015). Previous studies have established that excellent control of membrane voltage, including the T-tubule potential, is possible using short, small-diameter FDB fibers and TTX to block voltage-dependent sodium channels (Woods et al., 2004; DiFranco et al., 2005). Micropipettes were pulled from borosilicate glass capillaries (1.5 OD/0.86 ID) using a horizontal puller (P97; Sutter Instrument) to produce a steep taper and submicron tip diameter. Current injecting and voltage-recording electrodes were filled with intracellular solution and had resistances of 7–10 MΩ.

Fibers were impaled in the presence of standard Tyrode's solution under current-clamp conditions. Fibers initially had resting potentials of −30 to −50 mV and repolarized to −90 mV upon injection of a small steady current. The bath solution was then exchanged for 4K-EXT, and the fibers hyperpolarized to −120 to −130 mV as a result of the increased membrane resistance. The holding current was reduced as needed to maintain the membrane potential at −90 mV. An equilibration time of 20–30 min was allowed for the intracellular solution to equilibrate with the myoplasm (Woods et al., 2004). After this time, the intracellular ionic concentrations in the voltage-clamped region are estimated to be ∼94% of the pipette concentration (Woods et al., 2004). Then, the amplifier was switched to voltage-clamp mode at maximum gain. Except where indicated otherwise, the holding potential was maintained at −90 mV, close to the calculated potassium equilibrium potential in 4K-EXT. Na,K-ATPase–specific current, Ip, was identified as the current activated by extracellular K⁺ and inhibited by micromolar ouabain (see Results), and was expressed as microampere/square centimeter of cylindrical surface area. Currents were amplified and low-pass filtered (eight-pole Bessel; Frequency Devices) using either 1×, 5 kHz or 10×, 500 Hz gain and cutoff frequency. Pulse generation and data acquisition were performed using 16-bit D/A and A/D converters at 33 kHz and Labview software (National Instruments).

Measurement of K⁺ affinity using a membrane fraction from mouse skeletal muscle

A plasma membrane fraction enriched in surface sarcolemma and T-tubules was prepared using a modification of a published protocol (Rasmussen et al., 2008). This protocol enriches plasma membrane and removes most ATPase activity that is not contributed by the Na,K-ATPase. In brief, 700 mg of mixed hindlimb skeletal muscle was minced and homogenized using a Tissue Tearor (three bursts of 30 s; Biospec Products) in cold homogenization buffer containing 250 mM sucrose, 5 mM EGTA, 30 mM histidine, protease inhibitor cocktail (Sigma-Aldrich), and 0.1% deoxycholate, pH 6.8. The crude homogenate was centrifuged at 3,700 g for 15 min (4°C). The resultant supernatant was centrifuged at 200,000 g for 90 min (4°C). The final pellet containing a plasma membrane–enriched fraction was resuspended in solubilization buffer (1 mM imidazole and 1 mM EDTA) and used to assay enzyme activity. Protein concentration was measured using BSA Protein Assay Standards (Thermo Fisher Scientific). Protein yield was $2.51 \pm 0.82\%$ of the total protein content in the starting crude homogenate for wild-type samples, and $2.08 \pm 0.67\%$ for skα2⁻/⁻ samples. Fold purification of the Na,K-ATPase α1 and α2 isoforms was quantified by Western blot using isoform-specific antibodies. Fold purification of α1 and α2 in the wild-type membranes was 3.1 ± 1.5 and 4.6 ± 2.3, respectively; fold purification

of α1 in the skα2$^{-/-}$ membranes was 3.7 ± 1.9. Therefore, the recovery of α subunits in the wild-type membrane fraction (calculated as fold purification × total protein yield) was 7.8% for α1 and 11.54% for α2. Recovery of α1 in the skα2$^{-/-}$ membrane fraction was 7.7%. This recovery is comparable to published reports (Juel et al., 2013). The pooled mouse hindlimb skeletal muscles contain a majority of fast fiber types (Burkholder et al., 1994).

K$^+$-dependent Na,K-ATPase activity was determined from the amount of inorganic phosphate (Pi) released from samples incubated in different concentrations of K$^+$. A reaction mix was prepared containing 40 µl of 1 µg/µl protein and 160 µl of activity buffer (80 mM NaCl, 50 mM Tris-base, 5 mM EGTA, 5 mM MgCl$_2$, and various concentrations of KCl: 0, 2, 4, 6, 8, 10, 15, and 20 mM). Ionic strength was maintained by equimolar replacement of KCl with choline chloride. 2 mM ouabain was added to half of the samples from a concentrated stock. After a 15-min equilibration, the reaction was started by the addition of 0.5 mM Na$_2$-ATP (Sigma-Aldrich). The reaction was performed for 30 min. Then, 40 µl of each sample was transferred to four wells in a 96-well plate (10 µl per well), and the reaction was terminated by the addition of 250 µl Biomol Green reagent (Enzo Life Sciences) per well. The absorbance at 620 nM was measured (EnVision 2103 Multilabel Plate Reader; PerkinElmer) and used to compute the amount of Pi released using a standard curve. Pi released in K$^+$-free buffer, representing non–Na,K-ATPase–mediated ATPase activity, was 20% of total Pi and was subtracted to obtain the specific Na,K-ATPase activity. Pi release measured in K$^+$-free buffer was not significantly changed by the addition of 2 mM ouabain, confirming that K$^+$-dependent ATPase activity measured in this assay represents specific catalytic activity by the Na,K-ATPase.

Data analysis and statistics

Data were analyzed using Origin 8.0 (OriginLab) and Prism (Graph-Pad Software, Inc.) and reported as the mean or median value ± SEM. Differences between means were evaluated using the Student's t test with significance at P < 0.05. $K_{1/2,K}$ was obtained by fitting the measurements of peak Ip at different K$^+$ concentrations to the Hill equation,

$$\frac{Ip}{Ip_{max}} = \frac{[K]^h}{[K]^h + K_{1/2,K}{}^h},$$

where Ip_{max} is the maximum pump current, $[K]$ is the extracellular K$^+$ concentration, and $K_{1/2,K}$ is the K$^+$ concentration for half-activation

of peak Ip, and h is the Hill coefficient. ATPase activity measured in vitro was analyzed in the same way to obtain the maximum turnover rate, $Vmax$, and $K_{1/2,K}$.

RESULTS

Identification of Na,K-ATPase pump current in mouse FDB fibers

The Na,K-ATPase is a current-generating molecule. In its forward mode, the pump transports three Na$^+$ out and two K$^+$ ions into the cell per molecule of ATP hydrolyzed. This results in a net transfer of one positive charge per cycle that is detectable as an outward current. The coupling ratio three Na/two K/one ATP per pump cycle is constant over a wide range of conditions, including changes in intracellular Na$^+$ and ATP and extracellular K$^+$, and is independent of membrane potential (Glitsch, 2001).

Our experimental conditions were designed to favor forward pump transport in the absence of ion channel currents, in the context of physiological concentrations of extracellular Na$^+$ (114–154 mM) and intracellular K$^+$ (138 mM). The use of a high extracellular Na$^+$ concentration also minimizes proton current by the Na,K-ATPase, which increases in the absence of extracellular Na$^+$ (Vedovato and Gadsby, 2014). Fibers were voltage clamped near the physiological resting potential (−90 mV). Intracellular Na$^+$ (50 mM) was maintained at the upper end of values reported for contracting mouse muscles (Fong et al., 1986); additional Na$^+$ entry is reduced by the presence of TTX. A high intracellular Na$^+$ concentration reduces transient changes in Na$^+$ during the time the pump is either stopped or active, and keeps the intracellular-facing Na$^+$ sites of the enzyme near saturation. These conditions ensured that the change from a solution containing nominally 0 K (0K-EXT) to
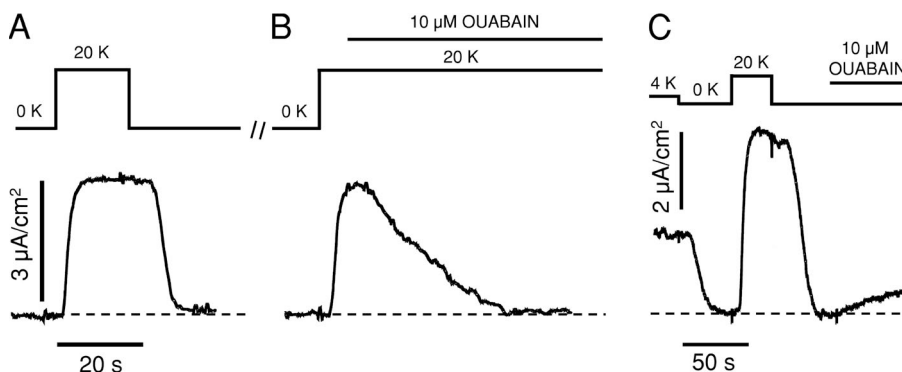
Figure 1. Measurement of Na,K-ATPase pump current in isolated mouse FDB fibers. Na,K-ATPase pump current is identified as the outward current activated by extracellular K$^+$ and inhibited by ouabain. (A) Outward currents are elicited upon changing the extracellular K$^+$ concentration from 0 to 20 mM. A return to 0K-EXT elicits a decrease in current, as expected if the Na,K-ATPase is stopped as a result of removal of the transported ion. Complete exchange of solutions was achieved in 2–5 s for this and subsequent figures. //, elapsed time of ∼2 min. (B) The addition of 10 µM ouabain after a subsequent change to 20K-EXT completely inhibits Ip. (C) The Na,K-ATPase contributes outward current at resting extracellular K$^+$. A change from 4K- to 0K-EXT elicits a decrease in current. A change to 20K-EXT elicits an outward current that disappears upon return to 0K-EXT. The application of ouabain after Ip is stopped in 0K-EXT elicits a smaller, slowly activating outward current that is attributed to a residual ouabain-insensitive potassium current. The holding potential was −90 mV, and the temperature was 22°C for all panels. The dashed lines represent the zero-level current in the presence of 0K-EXT.

one containing a given K$^+$ concentration (2K- to 40K-EXT) elicits an outward pump current that is caused by increased occupancy of extracellular K$^+$ sites.

Typical recordings of Na,K-ATPase pump current, Ip, are shown in Fig. 1. Each measurement of Ip is bracketed by a brief period in 0K-EXT to arrest pump turnover and obtain the zero current baseline. A change from 0K- to 20K-EXT activates an outward current, which is abolished completely upon return to 0K-EXT (Fig. 1 A). The direction of the current in the presence of a high extracellular K$^+$ concentration suggests that it is driven by an active mechanism, as in this condition, the electromotive force for potassium, EMF$_K$ = (V$_m$ − E$_K$), is inwardly directed (i.e., favoring passive K influx). The time course of pump activation and deactivation by extracellular K$^+$ is rapid and complete in less than 4 s. This is within the time required for extracellular solution changes (2–5 s) and diffusion into the T-tubules (2–3 s; Nakajima et al., 1973), which are the rate-limiting steps in our measurement. Cation binding and unbinding to the Na,K-ATPase occur within milliseconds (Heyse et al., 1994).

A second exposure to 20K-EXT activates a large, reproducible outward current (Fig. 1 B). The addition of 10 µM ouabain in the continued presence of 20K-EXT inhibits the outward current (complete block within 35 s; range of 11–40 s), confirming the identification of the K$^+$-dependent outward current as arising from the Na,K-ATPase. In rodent skeletal muscles, a concentration of

10 µM ouabain is expected to block >99% of Na,K-ATPase α2, which has a >100-fold greater affinity for ouabain than for α1 (Krivoi et al., 2003; Chibalin et al., 2012). The complete block of Ip by 10 µM ouabain indicates that the pump current measured in these conditions reports largely current contributed by the Na,K-ATPase α2. A small contribution of α1 is also expected from its low abundance in mouse fast-twitch fibers (13% of total α subunit; He et al., 2001) and the fact that α1 operates at 50–75% of its *Vmax* at resting extracellular K$^+$ concentration and the resting potential (Krivoi et al., 2003; Chibalin et al., 2012). Therefore, increases in Ip elicited by higher extracellular K$^+$ concentrations largely represent pump current generated by the α2 isoform.

Each bracketing change to 0K-EXT was kept to <30 s. When the pump is stopped in 0K-EXT, an increase in Donnan potential occurs, leading to increased intracellular Na$^+$ and fiber swelling. This phenomenon can produce an initial pump stimulation upon reintroduction of extracellular K$^+$ caused by greater occupancy of intracellular Na$^+$ sites. We determined empirically that this effect is minimized if the duration in 0K-EXT is kept to <30 s.

The Na,K-ATPase contributes a steady outward current at resting extracellular K$^+$, as expected (Fig. 1 C). This is evident as a decrease in current upon the initial change from 4K- to 0K-EXT. The outward current in 4K-EXT is approximately half that elicited by a subsequent change to 20K-EXT. The outward current disappears upon return to 0K-EXT. The addition of 10 µM ouabain to the 0K-EXT solution elicits a smaller outward current with slow kinetics that is attributed to a residual unblocked ionic current (EMF$_K$ is outward in 0K-EXT; see also Fig. 4). We considered whether a residual pump current might remain in the 0K-EXT solution
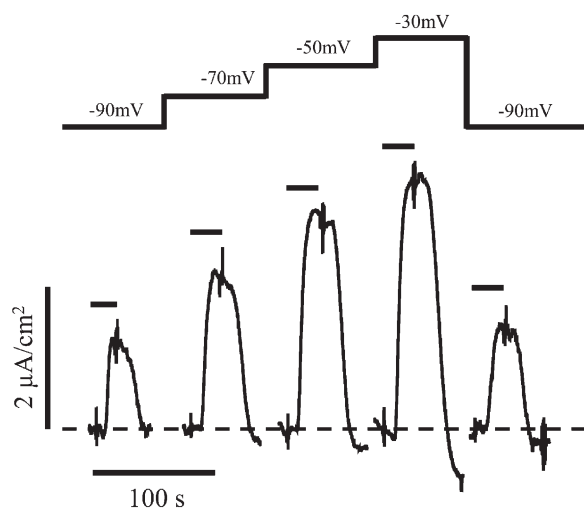
Figure 2. Voltage dependence of Ip. Representative Ip recordings obtained at different holding potentials from −90 to −30 mV, for a change from 0 K-EXT to 10 K-EXT solution. The approximate duration of the exposures to 10 mM K$^+$ is indicated above the current records. The holding potential between two consecutive levels was changed slowly over a period of ∼10 s. The schematic at the top of the panel indicates the imposed holding potentials, not the transitions between them. An additional period of 60–90 s was allowed before the [K$^+$] change was imposed. Individual Ip records are arbitrarily placed near each other. Temperature, 23°C.
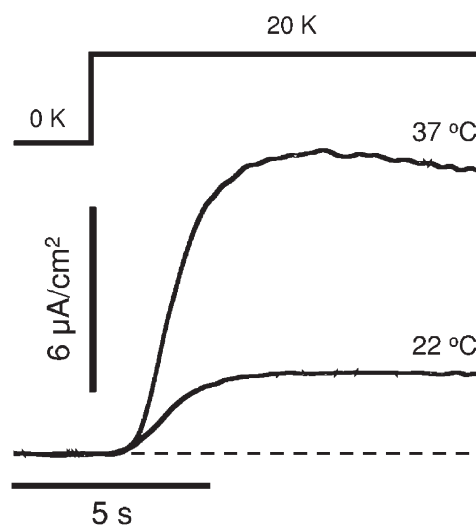
Figure 3. Effect of temperature on pump currents. Pump currents were measured at 22 and 37°C from the same fiber in response to a change from 0K-EXT to 20K-EXT. The record at 37°C was obtained 4 min after reaching a steady temperature reading.

if the K⁺ concentration in the T-tubules is not completely zero. However, this possibility is excluded because the α2 isoform, the only Na,K-ATPase in the T-tubules, is completely blocked by 10 μM ouabain.

The mean peak Ip at 20 mM of extracellular K⁺, −90 mV, and 22°C varied from 4 to 11 μA/cm², with a median value of 5.15 ± 0.64 μA/cm² of cylindrical surface area ($n = 15$).

Voltage dependence of Ip

Na,K-ATPase transport is voltage dependent. Pump currents are outward at all potentials in the physiological range, increasing from a negative equilibrium potential at which there is no net chemical reaction and therefore no ion transport (Rakowski et al., 1997; Glitsch, 2001).

In physiological concentrations of extracellular Na⁺, the voltage dependence arises largely from the effect of membrane potential on the unbinding and rebinding of Na⁺ to its extracellular binding site, which is accessed via a hydrophilic channel located within the membrane electric field (Gadsby et al., 1993; Rakowski et al., 1997; Glitsch, 2001). In cardiac myocytes perfused with extracellular Na⁺, the steepest voltage dependence occurs in the diastolic range of membrane potentials (−90 to −50 mV), and flattens at more depolarized potentials where the effect of membrane potential on Na⁺ binding is greatly reduced (Nakao and Gadsby, 1989).

In FDB fibers, peak Ip elicited by 10K-EXT is positive at all membrane potentials in the range of −90 to −30 mV (Fig. 2), increasing 1.5-fold ± 0.6 ($n = 5$) in the subthreshold
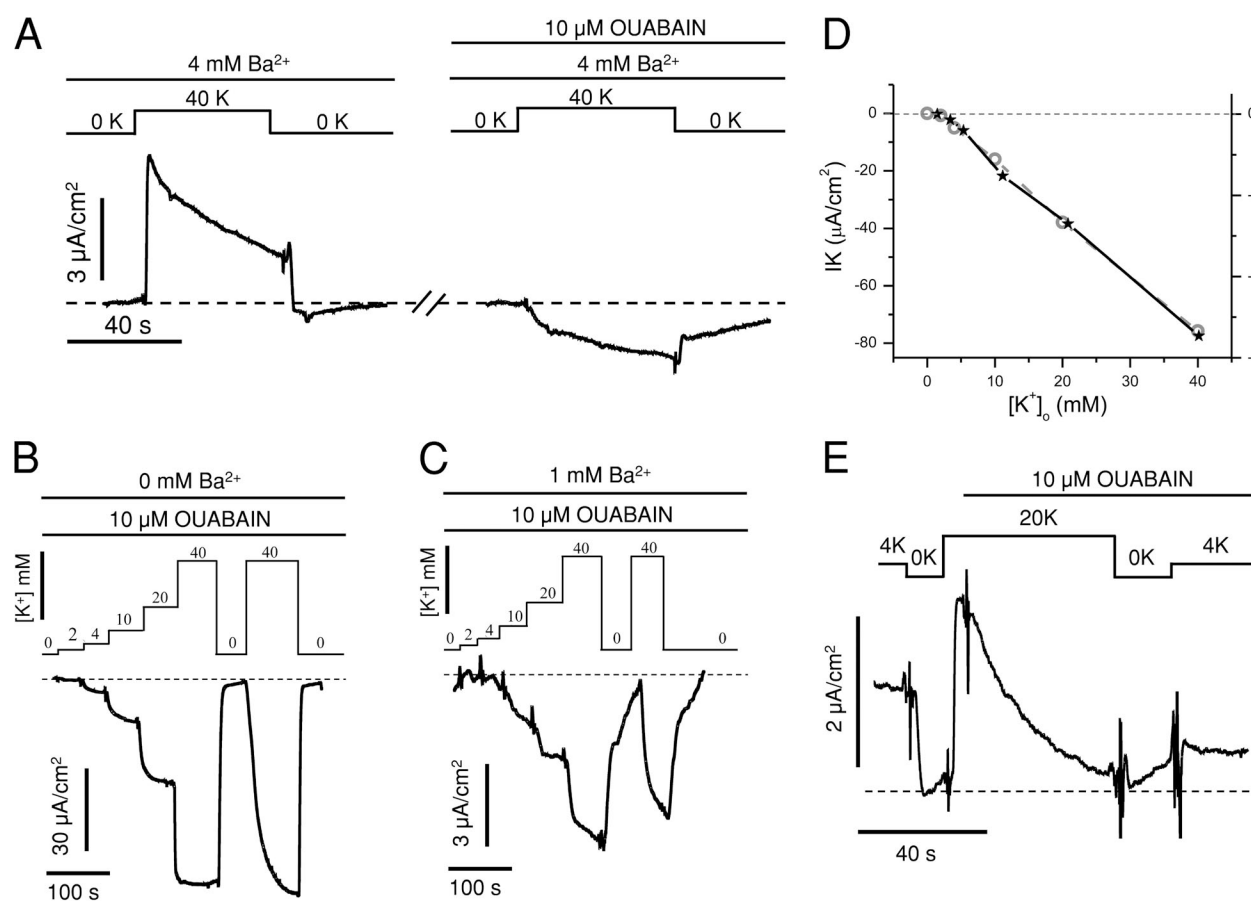
Figure 4. Contribution of ouabain-insensitive currents to measurements of Ip. (A) Example of Ip illustrating a pronounced current decay during exposure to a 40K-EXT solution (left), as seen in some experiments. The record also demonstrates an initial inward tail current upon the return to 0K-EXT. The addition of 10 μM ouabain reveals a slowly activating inward current in response to the same [K⁺] changes as in A (right). //, elapsed time of ∼2 min. (B) Ouabain-insensitive currents elicited by step changes in extracellular K⁺ concentration from 0 to 40 mM in the absence of Ba²⁺, and (C) in the presence of 1 mM Ba²⁺. Notice the differences in current scales. (D) Maximum ouabain-insensitive currents in B and C plotted as a function of the K⁺ concentration. Stars and circles represent ouabain-insensitive current measured in the absence of Ba²⁺ (left axis; circles and dashed lines) or in the presence of 1 mM Ba²⁺ (right axis; stars and solid lines), respectively. Note different y-axes scales. The ouabain-insensitive currents are inward at all K⁺ concentrations above 4 mM. (E) A change to 0K-EXT solution, in which E_K is outward, elicits a slowly activating outward current both in the absence (4K- to 0K-EXT change) and presence (20K- to 0K-EXT change) of 10 μM ouabain. The holding potential was −90 mV, and the temperature was 22°C for all panels. Dashed lines in all panels indicate the zero-current level in 0K-EXT. Data in A–C and E were obtained from three different fibers.

voltage range for action potential firing (-90 to -50). This result is comparable to the voltage dependence of the human recombinant $\alpha 2$ isozyme expressed in oocytes (Crambert et al., 2000) and the voltage dependence of the $\alpha 1$ isoform in cardiac myocytes (Gadsby et al., 1991).

Temperature dependence of Ip

Na,K-ATPase activity is highly temperature dependent, as expected for a vectorial enzyme reaction. To determine the Q_{10} for the $\alpha 2$ isoform in FDB fibers, we measured the currents elicited by extracellular K^+ concentrations from 0 to 20 mM in fibers acclimated (3–5 min) at 22 and 37°C (Fig. 3). In this example, peak Ip elicited by 20 mM K increased 3.7-fold upon raising the temperature to 37°C. The mean Q_{10} obtained from four similar experiments was 2.01 ± 0.12 ($n = 4$) over the temperature range of 22–37°C. This value compares closely with the Q_{10} of Na,K-ATPase current measured in rabbit sinoatrial node cells (Sakai et al., 1996), rat skeletal muscle (Clausen et al., 1987), and guinea pig arterial smooth muscle cells (Nakamura et al., 1999).

Contribution of other currents to measurement of Ip

It is often seen that current traces decay (Fig. 4 A) during exposure to constant extracellular K^+ concentrations, and they are followed by an initial inward tail current upon the return to 0K-EXT (left). The application of 10 µM ouabain uncovers a K^+-activated inward current having slow activation kinetics (Fig. 4 A, right). Only the outward pump current is blocked by ouabain. The inward currents are reduced but not completely eliminated by 4 mM Ba^{2+}. Fig. 4 (B and C) shows representative ouabain-insensitive currents elicited by various concentrations of K^+ in the absence or presence of 1 mM Ba^{2+}. Ba^{2+} concentrations above 4 mM did not produce further block. The ouabain-insensitive currents are inward for all K^+ concentrations above 4 mM (Fig. 4 D), as expected from the calculated EMF_K, which favors K^+ influx in 40K-EXT at -90 mV. Therefore, the slow inward current elicited by 40K-EXT at -90 mV and the initial tail current upon return to 0 K is attributed to a K current that is not completely blocked by millimolar Ba^{2+}. On the other hand, EMF_K is outward in 0K-EXT at -90 mV. If the ouabain-insensitive current originates from a residual unblocked potassium conductance, an outward current is expected in 0K-EXT solution, as can be seen in Fig. 4 E. For this fiber perfused in 4 mM of Ba^{2+}-containing extracellular solutions, a slow outward current is seen after the initial change from 4K- to 0K-EXT. The change to 20K-EXT elicits an initial fast-activating outward Ip, which is blocked by 10 µM ouabain. The return to 0K-EXT in the continued presence of ouabain elicits an initial fast inward tail current, followed
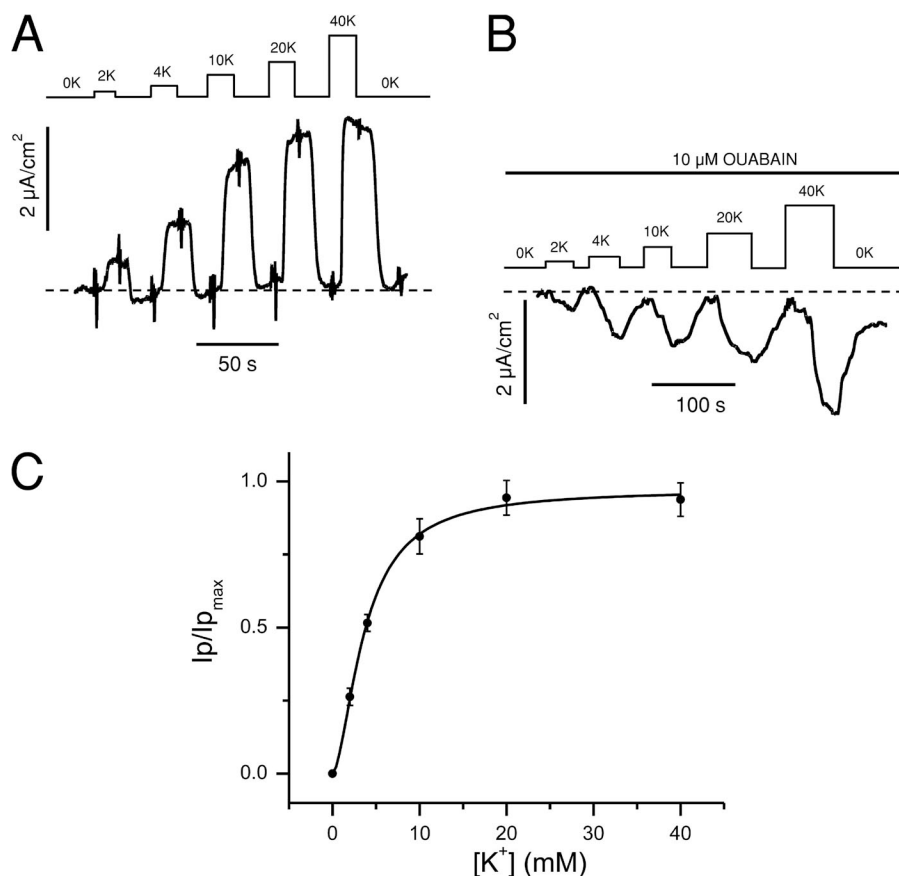
Figure 5. Apparent affinity of the Na,K-ATPase $\alpha 2$ isozyme for K^+. (A) Representative traces of Ip elicited by consecutive extracellular K^+ concentration changes from 0 to 2, 4, 10, 20, and 40 mM. (B) Current records from the same fiber after the addition of 10 µM ouabain. Current is plotted on same scale as A, but using a different time scale. The timing of the $[K^+]$ changes was approximated to align with the perfusion-dependent current artifacts. (C) Mean Ip values ($n = 18$ fibers) at each K^+ concentration were normalized to the mean Ip at 40 mM K^+ and fit to the Hill equation. The Hill coefficient was constrained to 1.68. Temperature, 22°C. Error bars represent mean $\pm$ SEM.

by a slowly activating outward current that is identical to the outward current seen at the initial change from 4K- to 0K-EXT. Based on its insensitivity to ouabain, dependence on E_K, slow kinetics, and sensitivity to block by Ba^{2+}, we tentatively attribute the K^+-activated, ouabain-insensitive current to residual potassium currents through inward rectifier channels (DiFranco et al., 2015). Inward rectifier channels are present at a high density in skeletal muscle T-tubules (Almers, 1980; Ashcroft et al., 1985; Kristensen and Juel, 2010; DiFranco et al., 2015). To avoid contributions from other currents in the determination of K^+ affinity, Ip was measured as the peak current immediately after reactivation of the Na,K-ATPase by extracellular K^+. At this time point, the maximum inward current in 40 mM K is <10% of peak Ip and was ignored.

The apparent K^+ affinity of the α2 isoform

The α2 isoform is the sole Na,K-ATPase isozyme in the T-tubules. Although extracellular K^+ is well equilibrated in all extracellular spaces under resting conditions, transient increases in the extracellular K^+ concentration in the T-tubules occur during electrical excitation. The excitation-dependent increases in lumen K^+ concentration depend on the frequency and duration of action potential activity. Therefore, we examined the activation of peak Ip by external K^+ over the range of K^+ concentrations expected in the T-tubules during sustained action potential excitation, while maintaining the membrane potential constant at −90 mV.

As shown in Fig. 4 D, peak Ip is not saturated at resting K^+ concentration (near 4 mM), but continues to increase up to 40 mM of extracellular K^+ (Fig. 5 A). In the absence of ouabain, peak Ip is reproducible during repeated changes in extracellular K^+ (not depicted). The addition of ouabain blocks the outward current at all K^+ concentrations, leaving only the potassium-dependent slow inward current (Fig. 5 B).

A fit of the mean peak Ip versus K^+ concentration data to the Hill equation reveals an apparent $K_{1/2,K}$ of 4.3 ± 0.3 mM ($n = 20$). Because the Hill coefficient is expected to be the same for all Na,K-ATPase isozymes and does not depend on the K^+ concentration, h was constrained to 1.68, the mean value obtained from an initial fit of all fibers. This value is consistent with measured values for the Na,K-ATPase with two extracellular K^+ sites (Jaisser et al., 1994). A $K_{1/2,K}$ of 4.3 mM indicates that the α2 isozyme operates near its $K_{1/2,K}$ at resting extracellular K^+ concentration and the resting potential, but can be significantly stimulated by further increases in extracellular K^+. Because cation binding is extremely fast and not rate limiting, stimulation of α2 activity by increased K^+ site occupancy will rapidly and dynamically follow the rise of extracellular K^+ concentration in the T-tubules that accompanies electrical activity.

This apparent $K_{1/2,K}$ value is likely an underestimate. Total Ip may contain a small outward pump current from α1, increasing in the range of 2–4 mM and constant thereafter; and Ip at high K^+ concentrations may be contaminated by inward currents. To estimate the error, if outward pump current from α1 contributes up to 25% of measured Ip at 4 mM K^+ and above, and inward currents reduce Ip by 25% at 40 mM K^+, removal of the combined effects will increase $K_{1/2,K}$ to up to 4.6 mM.

Voltage dependence of K^+ affinity

The apparent affinity for K^+ is not expected to be strongly voltage dependent in our conditions because the effect of membrane potential on Na^+ translocation dominates at physiological concentrations of extracellular Na^+. Any effects on K^+ affinity are expected to be small and apparent only at more positive membrane potentials where the effects of Na^+ are reduced (Gadsby and Nakao, 1989). Consistent with this expectation, the $K_{1/2,K}$ for the mouse FDB fibers is relatively voltage independent for membrane potentials from −90 to −30 mV (Fig. 6). There may be a tendency for $K_{1/2,K}$ to increase at more depolarized potentials, but this region was not explored because of unblocked ionic currents.

K^+ affinity measured in vitro

As an independent measure of the relative K^+ affinities of the α isoforms in skeletal muscle, we measured ATPase turnover in vitro using a microsome fraction enriched in surface and T-tubule membranes (Kristensen et al., 2008). Membranes were prepared from hindlimb skeletal muscles of wild-type mice and mice having a
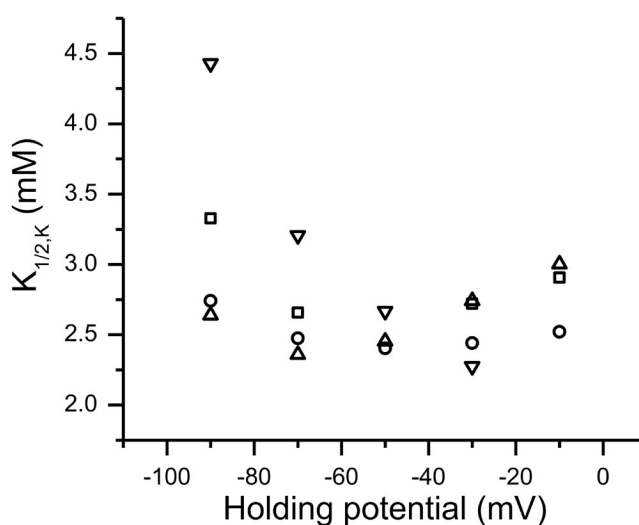
Figure 6. Voltage dependence of $K_{1/2,K}$. Apparent K^+ affinity was determined as shown in Fig. 5 C. Ip was measured in four fibers for five extracellular K^+ concentrations (2, 4, 10, 20, and 40 mM) and five holding potentials, and fit to the Hill equation to obtain $K_{1/2,K}$ values for each holding potential. The Hill coefficient was constrained to 1.68. Different symbols represent different fibers. Temperature, 22°C.

targeted knockout of the α2 isoform in the skeletal muscles (skα2$^{-/-}$; Radzyukevich et al., 2013). Wild-type skeletal muscles express both α1 and α2 isoforms, with α2 representing up to 90% of total α subunit, whereas skα2$^{-/-}$ muscles express only the α1 subunit at 2.5-fold greater level than control (Radzyukevich et al., 2013).

The $K_{1/2,K}$ of skα2$^{-/-}$ membranes was 1.7 ± 0.6 mM (Fig. 7). This is in the range of K$^+$ affinity values for the rodent and human α1 isoform measured in various cells and expression systems (Blanco and Mercer, 1998; Crambert et al., 2000; Glitsch, 2001; Blanco, 2005). On the other hand, the $K_{1/2,K}$ of wild-type membranes was significantly higher (3.6 ± 0.5 mM; n = 5; P < 0.04) and closer to the K$^+$ affinity of peak α2 pump current. A higher $K_{1/2,K}$ for the wild-type membranes is expected if the α2 isoform has a lower affinity for K$^+$ than α1.

DISCUSSION

The major new finding of this study is that the affinity of the Na,K-ATPase α2 isoform for K$^+$ is lower than that of α1, and matched to the range of K$^+$ concentrations that occur in the T-tubules during sustained activity. Therefore, the α2 isozyme in skeletal muscle operates below its maximum activity at resting extracellular [K$^+$] (4.3 mM for male C57/B6 mice; Boehm et al., 2007), conserving ATP, whereas during action potential activity, α2 activity can be rapidly increased in proportion to the K$^+$ concentration in the T-tubules. At constant membrane potential and near saturating intracellular Na$^+$, a two- to threefold increase in α2 activity above its rate in resting muscle can be achieved from increased K$^+$ site occupancy.

The apparent K$^+$ affinity constant for the α2 isozyme, obtained from the K$^+$ dependence of Ip, is 4.3 mM. This value represents a lower limit for the $K_{1/2,K}$ of α2. It is based on measurement of total Ip in the context of physiological concentration ranges for Na$^+$ and K$^+$, expected in quiescence or high levels of activity, and assumes that Ip represents largely pump current from α2.

However, Ip values may contain contributions from outward α1 pump current, which saturates at ~4 mM, and may be contaminated by inward ionic currents at high K$^+$ concentrations. A reasonable estimate of these errors may extend the $K_{1/2,K}$ of α2 up to 4.6 mM.

This finding provides a mechanistic explanation for previous observations that the α2 isozyme operates significantly below its maximal transport capacity in resting muscles (Krivoi et al., 2003; Radzyukevich et al., 2004; Chibalin et al., 2012), but that its activity can be rapidly increased by working muscles to maintain excitation and contraction (Radzyukevich et al., 2013).

This apparent affinity is lower than previously assumed. However, a lower K$^+$ affinity extends the regulatory range for stimulation of α2 activity by K$^+$ site occupancy, enabling it to increase when extracellular K$^+$ rises above resting levels. The physiological mode of muscle activation is repetitive action potential stimulation. Although the amount of K$^+$ that exits a muscle fiber during a single action potential is negligible, the cumulative effect into a diffusion-limited space can be significant. Extracellular K$^+$ in the T-tubules increases in direct proportion to the frequency and duration of action potential activity. During intense excitation, the T-tubule K$^+$ concentration can transiently reach tens of millimolar, with gradients of concentration between peripheral and central regions. Therefore, stimulation of α2 by luminal K$^+$ dynamically and spatially matches its transport activity to the intensity of muscle excitation.

A $K_{1/2,K}$ near 4 mM implies that the K$^+$ sites on α2 saturate in the range of 20–40 mM. This is significant because uniform exposure of muscle fibers to K$^+$ at these concentrations would reduce the membrane potential to values that lead to maximal slow inactivation of Na$^+$ channels and thereby blockage of action potential generation.

Stimulation of α2 in the T-tubules helps maintain membrane excitability in two ways. Because Na,K-ATPase transport is electrogenic, α2 activity provides an outward current that hyperpolarizes the membrane potential; at the same time, it returns extracellular K$^+$ to the
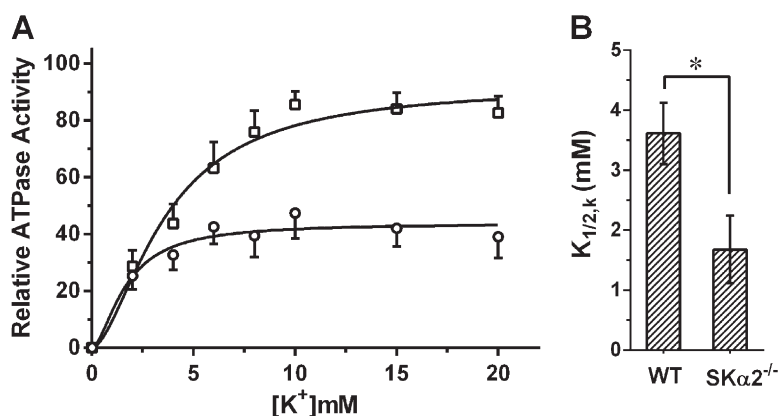
Figure 7. Apparent K$^+$ affinity of the Na,K-ATPase α2 isoform measured in membranes prepared from wild-type and skα2$^{-/-}$ mice. (A) Mean ATPase activity versus [K$^+$] for skeletal muscle membranes prepared from five wild-type (□) and four skα2$^{-/-}$ (○) mice. Solid lines are fits of the data to the Hill equation, with the Hill coefficient constrained to 1.68. (B) Mean fitted $K_{1/2,K}$ values for wild-type and skα2$^{-/-}$ muscle preparations. *, significant difference at P < 0.04. Na$^+$ concentration was fixed at 80 mM, and K$^+$ concentration was varied from 0 to 20 mM by equimolar replacement with choline chloride. Temperature, 22°C. Error bars represent mean ± SEM.

cytosol (and removes intracellular Na^+) to restore the ion gradients and reset the Nernst potential for potassium to its resting value. The electrogenic hyperpolarizing action is immediate, whereas full restoration of the K^+ and Na^+ concentrations can take minutes or longer (Clausen, 2003b).

$K_{1/2,K}$ is relatively voltage independent at membrane potentials in the range of -90 to -30 mV, and may tend to increase at more depolarized potentials. Whether this property has any physiological consequence is not immediately apparent. A steady depolarization of the Nernst potential to voltages above -50 mV would inactivate excitation–contraction coupling before any effects on Na,K-ATPase activity could be realized.

Notably, the affinity of $\alpha 2$ for K^+ is significantly lower than that of $\alpha 1$. The good agreement between the electrophysiological and biochemical determinations of $K_{1/2,K}$ in muscles from the same wild-type mice, and the significantly higher K^+ affinity in muscles that express only $\alpha 1$, further supports our conclusion that the ouabain-sensitive current is generated largely by the $\alpha 2$ Na,K-ATPase.

Acute, excitation-related stimulation of the $\alpha 2$ isoform

This study focused on the acute, excitation-related stimulation of Na,K-ATPase $\alpha 2$ by extracellular K^+ and membrane potential, under conditions of elevated intracellular Na^+ and reduced Na^+ entry. However, during normal muscle activation, Na^+ influx during repetitive action potential activity also stimulates the Na,K-ATPase by increasing the occupancy of intracellular Na^+ sites (Clausen, 2003b). All of these effects—increased occupancy of both K^+ and Na^+ sites, depolarization, and increased temperature—will combine synergistically in a direction to increase Na,K-ATPase $\alpha 2$ activity immediately upon the start of membrane excitation. Additional stimulation of Na,K-ATPase activity can occur from hormonal and other inputs, depending on contractile conditions (Clausen, 2003b, 2013).

Measurement of pump currents in single muscle fibers

This study defines conditions for reliably recording a K^+-activated, ouabain-sensitive outward current that largely reports forward cycling of the Na,K-ATPase $\alpha 2$ isozyme. The proportional contribution of $\alpha 2$ to the total pump current is expected to increase with increasing extracellular K^+, reaching up to 90% of total pump current at K^+ concentrations >20 mM. This is the first measurement of Na,K-ATPase pump currents in voltage-clamped single skeletal muscle fibers, and the first measurement of the apparent K^+ affinity of the $\alpha 2$ isozyme in intact muscle cells.

This approach affords important advantages for studies of the Na,K-ATPase isoforms in skeletal muscle. Although expression systems and purified membranes have been indispensable for uncovering the biophysical properties of the Na,K-ATPase, they are conducted under very artificial conditions. To fully appreciate the functional significance of the different isoforms, it is important to examine them in a more physiological context. Voltage clamping of single muscle fibers has advantages over measurements of K^+ affinity in whole muscles, which are limited by diffusion delays in the interstitial spaces (Clausen et al., 1987) and the inability to impose extracellular K^+ concentration changes without simultaneously changing the membrane potential. Voltage-clamp studies on single muscle fibers made it possible to impose extracellular K^+ concentration changes at constant membrane potential, with rapid equilibration of extracellular solutions, and stable, near saturating intracellular Na^+ concentration. Our approach will enable future studies of Na,K-ATPase regulation in live fibers with high time resolution and sensitive detection.

Physiological significance

The findings in this study suggest that the K^+ affinities of the $\alpha 1$ and $\alpha 2$ isozymes are set to operate over different ranges of extracellular K^+ concentrations. The K^+ affinity and localization of $\alpha 1$ in the outer sarcolemma (Williams et al., 2001) position it to handle the range of K^+ concentrations that exist in the muscle interstitial spaces at rest and during contraction (4–10 mM; Radzyukevich et al., 2009). The K^+ affinity of the $\alpha 1$ isoform has not been measured in intact skeletal muscles, but a reasonable estimate can be inferred from measurements in other preparations. Rodent cardiac muscles that express mainly $\alpha 1$ (Glitsch, 2001), recombinant $\alpha 1$ isozymes expressed in oocytes (Crambert et al., 2000), and skeletal muscle membranes having only the $\alpha 1$ isoform (this study) all have a half-activation constant for K^+ in the 1–2-mM range. For this affinity, the $\alpha 1$ isoform in skeletal muscle is expected to operate significantly above its $K_{1/2,K}$ at resting extracellular K^+ concentration. This expectation is supported by experimental evidence. Measurements of the hyperpolarization contributed by $\alpha 1$ electrogenic transport at resting extracellular K^+ indicate that $\alpha 1$ operates above its $K_{1/2,K}$ and provides a majority of the basal Na^+/K^+ transport needed to maintain resting ion gradients and the resting potential (Krivoi et al., 2003; Chibalin et al., 2012). Skeletal muscles with 50% reduced $\alpha 2$ content maintain normal ion gradients (He et al., 2001), and skeletal muscles without any $\alpha 2$ maintain near normal resting potentials (Radzyukevich et al., 2004, 2013). These considerations indicate that the $\alpha 1$ isoform in skeletal muscle performs the canonical role of the Na,K-ATPase in setting ion gradients and the resting potential. However, because $\alpha 1$ operates in the upper end of its regulatory range for activation by K^+, its capacity for further stimulation by extracellular K^+ is limited.

The $\alpha 2$ isoform in skeletal muscle does not make a major contribution to these canonical Na,K-ATPase roles. Its K^+ affinity and localization in caveolae and

T-tubules, where it is the sole α isoform, position it to respond to the K⁺ concentration increases that occur during membrane excitation. Therefore, α2 provides a reserve transport capacity that can be rapidly recruited to meet the demand of working muscles for increased Na⁺/K⁺ transport (Fig. 8).

The molecular determinants of K⁺ affinity are not completely known. The K⁺ affinity of the α1 and α2 isozymes is similar when paired with the same β isoform (Jewell and Lingrel, 1991), suggesting that their different K⁺ affinities are not conferred solely by the α subunit. Studies of recombinant rodent (Blanco and Mercer, 1998) and human α-β heteromers (Crambert et al., 2000; Geering, 2008) suggest that the β subunit, a single spanning membrane protein important in targeting and stabilization, can influence K⁺ affinity through a cooperative interaction with the α subunit. In both rodents and humans, an α1 or α2 subunit combined with β2 has a lower K⁺ affinity than either α subunit combined with β1. The recombinant rodent α2-β2 expressed in insect cells and the recombinant human α2-β2 expressed in oocytes have apparent K⁺ affinities of 4.8 mM (Blanco and Mercer, 1998) and 2.7 mM (Crambert et al., 2000), respectively. Structural studies of the shark enzyme strongly suggest that the β subunit has a critical role in K⁺ binding (Shinoda et al., 2009). The K⁺-binding sites on the α subunit are located near transmembrane helices M4 and M5. Binding of K⁺ to these sites is predicted to cause large-scale

structural changes on transmembrane helices M7–M10, which align near and interact with the β subunit. Rodent skeletal muscles express β1, β2, and β3, although not all muscle types express β3 (Hundal et al., 1993; He et al., 2001; Cougnon et al., 2002; Ng et al., 2003). In the brain, the β2 subunit is a preferred partner of α2 (Tokhtaeva et al., 2012). The β-subunit partner(s) of α2 and the subcellular localization of β subunits in skeletal muscle are not known. Different combinations of α-β heteromers are likely to exist in different fiber types because the β isoforms show a preferred fiber-type expression. Fast glycolytic fibers express largely β2, whereas slow oxidative fiber types express largely β1 (Hundal et al., 1993; Fowles et al., 2004; Zhang et al., 2006). If more than one β isoform is present in the T-tubules, it is possible that multiple α2-β isozymes exist, which could provide another level of complexity. Additional information on β-subunit expression, distribution, and membrane localization in skeletal muscle will be needed to determine the functional roles of the different α2-β isozymes.

In addition to the β subunit, the α2 subunit also partners with the FXYD1 subunit (also termed "phospholemman") in mouse skeletal muscles (Chibalin et al., 2012). Phospholemman influences enzyme activity by increasing the affinity for intracellular Na⁺ and/or increasing the maximum turnover rate (Geering, 2008), and it may also induce a small decrease in the K⁺ affinity of both isoforms (Crambert et al., 2000; Li et al., 2004).
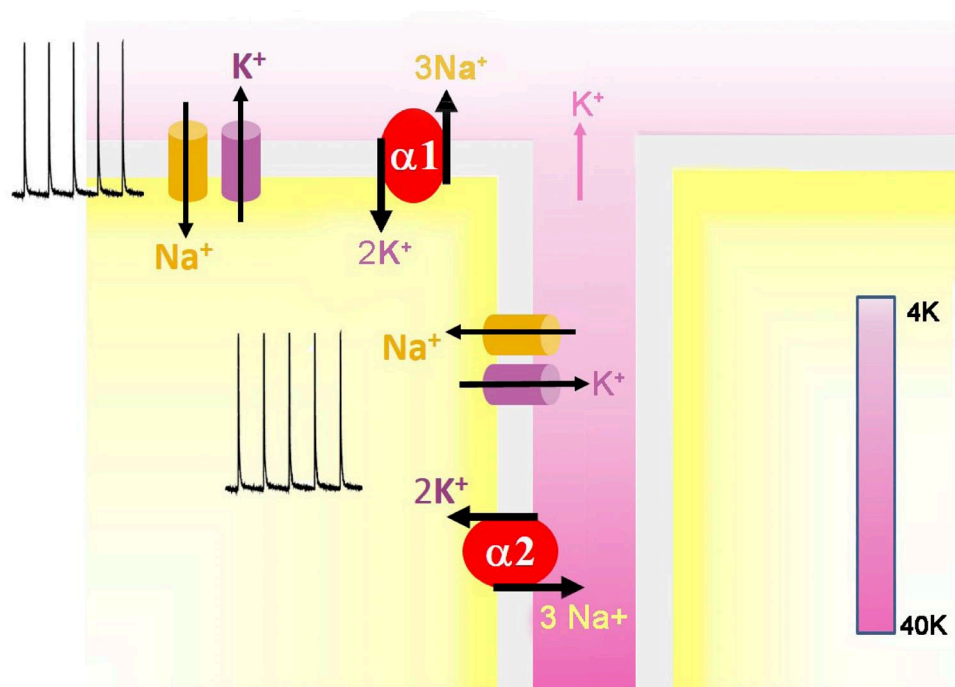
Figure 8. Model: The α1 and α2 isoforms of the Na,K-ATPase in skeletal muscles operate over different ranges of extracellular K⁺ concentrations. During repetitive action potential activity, extracellular K⁺ increases up to 10–12 mM in the muscle interstitial spaces and can reach tens of millimolar in the T-tubules. Increased K⁺ rapidly stimulates the activity of both isoforms by increasing the occupancy of the extracellular K⁺ sites of the enzyme. The α1 isoform, localized in the outer sarcolemma, operates above its $K_{1/2,K}$ (1–2 mM) at resting extracellular [K⁺] (4 mM), and plays a major role in setting resting ion gradients and the resting potential. The α2 isoform is the sole Na,K-ATPase in the T-tubules. It operates below its maximum activity in resting muscles, but its activity can be rapidly increased during membrane excitation to meet the increased demands of working muscle for Na/K transport. The cartoon emphasizes the spatial segregation and different $K_{1/2,K}$ constants of α1 and α2 isoforms, which match the range of [K⁺] expected at rest and during activity. The model also suggests that a small fraction of the K⁺ can diffuse out of the tubular system through the tubule openings. For simplicity, only voltage-dependent sodium and potassium channels (Nav1.4 and Kv1.4/Kv3.4) are indicated. Kir channels are also expected to contribute to the recovery of K⁺, because the electromotive force for K⁺ is inward above 4 mM [K⁺]ₒ.

In summary, the α2 Na,K-ATPase in skeletal muscle, the sole Na,K-ATPase isoform in the T-tubules, can be stimulated by K^{+} over a regulatory range, which allows it to respond to T-tubular lumen (extracellular) K^{+} concentrations up to 40 mM. Results of this study may be relevant to other excitable cell types and/or membrane domains that express the Na,K-ATPase α2 isoform and experience large changes in extracellular K^{+}.

REFERENCES

Almers, W. 1980. Potassium concentration changes in the transverse tubules of vertebrate skeletal muscle. *Fed. Proc.* 39:1527–1532.

Ashcroft, F.M., J.A. Heiny, and J. Vergara. 1985. Inward rectification in the transverse tubular system of frog skeletal muscle studied with potentiometric dyes. *J. Physiol.* 359:269–291. http://dx.doi.org/10.1113/jphysiol.1985.sp015585

Berry, R.G., S. Despa, W. Fuller, D.M. Bers, and M.J. Shattock. 2007. Differential distribution and regulation of mouse cardiac Na^{+}/K^{+}-ATPase alpha1 and alpha2 subunits in T-tubule and surface sarcolemmal membranes. *Cardiovasc. Res.* 73:92–100. http://dx.doi.org/10.1016/j.cardiores.2006.11.006

Blanco, G. 2005. Na,K-ATPase subunit heterogeneity as a mechanism for tissue-specific ion regulation. *Semin. Nephrol.* 25:292–303. http://dx.doi.org/10.1016/j.semnephrol.2005.03.004

Blanco, G., and R.W. Mercer. 1998. Isozymes of the Na-K-ATPase: heterogeneity in structure, diversity in function. *Am. J. Physiol.* 275:F633–F650.

Boehm, O., B. Zur, A. Koch, N. Tran, R. Freyenhagen, M. Hartmann, and K. Zacharowski. 2007. Clinical chemistry reference database for Wistar rats and C57/BL6 mice. *Biol. Chem.* 388:547–554. http://dx.doi.org/10.1515/BC.2007.061

Burke, R.E., D.N. Levine, P. Tsairis, and F.E. Zajac III. 1973. Physiological types and histochemical profiles in motor units of the cat gastrocnemius. *J. Physiol.* 234:723–748. http://dx.doi.org/10.1113/jphysiol.1973.sp010369

Burkholder, T.J., B. Fingado, S. Baron, and R.L. Lieber. 1994. Relationship between muscle fiber types and sizes and muscle architectural properties in the mouse hindlimb. *J. Morphol.* 221:177–190. http://dx.doi.org/10.1002/jmor.1052210207

Chibalin, A.V., J.A. Heiny, B. Benziane, A.V. Prokofiev, A.V. Vasiliev, V.V. Kravtsova, and I.I. Krivoi. 2012. Chronic nicotine modifies skeletal muscle Na,K-ATPase activity through its interaction with the nicotinic acetylcholine receptor and phospholemman. *PLoS ONE.* 7:e33719. http://dx.doi.org/10.1371/journal.pone.0033719

Clausen, T. 2003a. Effects of age and exercise training on Na^{+}-K^{+} pumps in skeletal muscle. *Am. J. Physiol. Regul. Integr. Comp. Physiol.* 285:R720–R721. http://dx.doi.org/10.1152/ajpregu.00357.2003

Clausen, T. 2003b. Na^{+}-K^{+} pump regulation and skeletal muscle contractility. *Physiol. Rev.* 83:1269–1324. http://dx.doi.org/10.1152/physrev.00011.2003

Clausen, T. 2013. Quantification of Na^{+},K^{+} pumps and their transport rate in skeletal muscle: Functional significance. *J. Gen. Physiol.* 142:327–345.

Clausen, T., M.E. Everts, and K. Kjeldsen. 1987. Quantification of the maximum capacity for active sodium-potassium transport in rat skeletal muscle. *J. Physiol.* 388:163–181. http://dx.doi.org/10.1113/jphysiol.1987.sp016608

Cougnon, M.H., A.E. Moseley, T.L. Radzyukevich, J.B. Lingrel, and J.A. Heiny. 2002. Na,K-ATPase α- and β-isoform expression in developing skeletal muscles: α2 correlates with t-tubule formation. *Pflugers Arch.* 445:123–131.

Crambert, G., U. Hasler, A.T. Beggah, C. Yu, N.N. Modyanov, J.D. Horisberger, L. Lelièvre, and K. Geering. 2000. Transport and pharmacological properties of nine different human Na, K-ATPase isozymes. *J. Biol. Chem.* 275:1976–1986. http://dx.doi.org/10.1074/jbc.275.3.1976

DiFranco, M., J. Capote, and J.L. Vergara. 2005. Optical imaging and functional characterization of the transverse tubular system of mammalian muscle fibers using the potentiometric indicator di-8-ANEPPS. *J. Membr. Biol.* 208:141–153. http://dx.doi.org/10.1007/s00232-005-0825-9

DiFranco, M., C. Yu, M. Quiñonez, and J.L. Vergara. 2015. Inward rectifier potassium currents in mammalian skeletal muscle fibres. *J. Physiol.* 593:1213–1238. http://dx.doi.org/10.1113/jphysiol.2014.283648

Edman, K.A. 2005. Contractile properties of mouse single muscle fibers, a comparison with amphibian muscle fibers. *J. Exp. Biol.* 208:1905–1913. http://dx.doi.org/10.1242/jeb.01573

Eisenberg, B.R., and A.M. Kuda. 1975. Stereological analysis of mammalian skeletal muscle: II. White vastus muscle of the adult guinea pig. *J. Ultrastruct. Res.* 51:176–187. http://dx.doi.org/10.1016/S0022-5320(75)80146-8

Eltit, J.M., X. Ding, I.N. Pessah, P.D. Allen, and J.R. Lopez. 2013. Nonspecific sarcolemmal cation channels are critical for the pathogenesis of malignant hyperthermia. *FASEB J.* 27:991–1000. http://dx.doi.org/10.1096/fj.12-218354

Everts, M.E., and T. Clausen. 1994. Excitation-induced activation of the Na^{+}-K^{+} pump in rat skeletal muscle. *Am. J. Physiol.* 266:C925–C934.

Fong, C.N., H.L. Atwood, and M.P. Charlton. 1986. Intracellular sodium-activity at rest and after tetanic stimulation in muscles of normal and dystrophic (dy2J/dy2J) C57BL/6J mice. *Exp. Neurol.* 93:359–368. http://dx.doi.org/10.1016/0014-4886(86)90196-2

Fowles, J.R., H.J. Green, and J. Ouyang. 2004. Na^{+}-K^{+}-ATPase in rat skeletal muscle: content, isoform, and activity characteristics. *J. Appl. Physiol.* 96:316–326. http://dx.doi.org/10.1152/japplphysiol.00745.2002

Fraser, J.A., C.L. Huang, and T.H. Pedersen. 2011. Relationships between resting conductances, excitability, and t-system ionic homeostasis in skeletal muscle. *J. Gen. Physiol.* 138:95–116. http://dx.doi.org/10.1085/jgp.201110617

Froehlich, J.P., and K. Fendler. 1991. The partial reactions of the Na^{+}- and Na^{+} + K^{+}-activated adenosine triphosphatases. *Soc. Gen. Physiol. Ser.* 46:227–247.

Gadsby, D.C., and M. Nakao. 1989. Steady-state current-voltage relationship of the Na/K pump in guinea pig ventricular myocytes. *J. Gen. Physiol.* 94:511–537. http://dx.doi.org/10.1085/jgp.94.3.511

Gadsby, D.C., M. Nakao, and A. Bahinski. 1991. Voltage-induced Na/K pump charge movements in dialyzed heart cells. *Soc. Gen. Physiol. Ser.* 46:355–371.

Gadsby, D.C., R.F. Rakowski, and P. De Weer. 1993. Extracellular access to the Na,K pump: Pathway similar to ion channel. *Science.* 260:100–103. http://dx.doi.org/10.1126/science.7682009

Geering, K. 2008. Functional roles of Na,K-ATPase subunits. *Curr. Opin. Nephrol. Hypertens.* 17:526–532. http://dx.doi.org/10.1097/MNH.0b013e3283036cbf

Glitsch, H.G. 2001. Electrophysiology of the sodium-potassium-ATPase in cardiac cells. *Physiol. Rev.* 81:1791–1826.

Green, H.J. 2004. Mechanisms and management of fatigue in health and disease: Symposium introduction. *Can. J. Appl. Physiol.* 29:264–273. http://dx.doi.org/10.1139/h04-018

He, S., D.A. Shelly, A.E. Moseley, P.F. James, J.H. James, R.J. Paul, and J.B. Lingrel. 2001. The α_1- and α_2-isoforms of Na-K-ATPase play different roles in skeletal muscle contractility. *Am. J. Physiol. Regul. Integr. Comp. Physiol.* 281:R917–R925.

Hennig, R., and T. Lømo. 1985. Firing patterns of motor units in normal rats. *Nature.* 314:164–166. http://dx.doi.org/10.1038/314164a0

Heyse, S., I. Wuddel, H.J. Apell, and W. Stürmer. 1994. Partial reactions of the Na,K-ATPase: determination of rate constants. *J. Gen. Physiol.* 104:197–240. http://dx.doi.org/10.1085/jgp.104.2.197

Hundal, H.S., A. Marette, T. Ramlal, Z. Liu, and A. Klip. 1993. Expression of beta subunit isoforms of the Na$^+$,K$^+$-ATPase is muscle type-specific. *FEBS Lett.* 328:253–258. http://dx.doi.org/10.1016/0014-5793(93)80938-Q

Jaisser, F., P. Jaunin, K. Geering, B.C. Rossier, and J.D. Horisberger. 1994. Modulation of the Na,K-pump function by β subunit isoforms. *J. Gen. Physiol.* 103:605–623. http://dx.doi.org/10.1085/jgp.103.4.605

Jewell, E.A., and J.B. Lingrel. 1991. Comparison of the substrate dependence properties of the rat Na,K-ATPase alpha 1, alpha 2, and alpha 3 isoforms expressed in HeLa cells. *J. Biol. Chem.* 266:16925–16930.

Juel, C. 1988. The effect of beta 2-adrenoceptor activation on ion-shifts and fatigue in mouse soleus muscles stimulated in vitro. *Acta Physiol. Scand.* 134:209–216. http://dx.doi.org/10.1111/j.1748-1716.1988.tb08481.x

Juel, C., N.B. Nordsborg, and J. Bangsbo. 2013. Exercise-induced increase in maximal in vitro Na-K-ATPase activity in human skeletal muscle. *Am. J. Physiol. Regul. Integr. Comp. Physiol.* 304:R1161–R1165. http://dx.doi.org/10.1152/ajpregu.00591.2012

Kaplan, J.H. 2002. Biochemistry of Na,K-ATPase. *Annu. Rev. Biochem.* 71:511–535. http://dx.doi.org/10.1146/annurev.biochem.71.102201.141218

Kirsch, G.E., R.A. Nichols, and S. Nakajima. 1977. Delayed rectification in the transverse tubules: origin of the late after-potential in frog skeletal muscle. *J. Gen. Physiol.* 70:1–21. http://dx.doi.org/10.1085/jgp.70.1.1

Kristensen, M., and C. Juel. 2010. Potassium-transporting proteins in skeletal muscle: cellular location and fibre-type differences. *Acta Physiol. (Oxf.).* 198:105–123. http://dx.doi.org/10.1111/j.1748-1716.2009.02043.x

Kristensen, M., M.K. Rasmussen, and C. Juel. 2008. Na$^+$-K$^+$ pump location and translocation during muscle contraction in rat skeletal muscle. *Pflugers Arch.* 456:979–989. http://dx.doi.org/10.1007/s00424-008-0449-x

Krivoi, I., A. Vasiliev, V. Kravtsova, M. Dobretsov, and F. Mandel. 2003. Porcine kidney extract contains factor(s) that inhibit the ouabain-sensitive isoform of Na,K-ATPase (α2) in rat skeletal muscle: A convenient electrophysiological assay. *Ann. NY Acad. Sci.* 986:639–641. http://dx.doi.org/10.1111/j.1749-6632.2003.tb07272.x

Li, C., A. Grosdidier, G. Crambert, J.D. Horisberger, O. Michielin, and K. Geering. 2004. Structural and functional interaction sites between Na,K-ATPase and FXYD proteins. *J. Biol. Chem.* 279:38895–38902. http://dx.doi.org/10.1074/jbc.M406697200

Nakajima, S., Y. Nakajima, and L.D. Peachey. 1973. Speed of repolarization and morphology of glygerol-treated frog muscle fibres.

J. Physiol. 234:465–480. http://dx.doi.org/10.1113/jphysiol.1973.sp010355

Nakamura, Y., Y. Ohya, I. Abe, and M. Fujishima. 1999. Sodium-potassium pump current in smooth muscle cells from mesenteric resistance arteries of the guinea-pig. *J. Physiol.* 519:203–212. http://dx.doi.org/10.1111/j.1469-7793.1999.0203o.x

Nakao, M., and D.C. Gadsby. 1989. [Na] and [K] dependence of the Na/K pump current-voltage relationship in guinea pig ventricular myocytes. *J. Gen. Physiol.* 94:539–565. http://dx.doi.org/10.1085/jgp.94.3.539

Ng, Y.C., M. Nagarajan, K.N. Jew, L.C. Mace, and R.L. Moore. 2003. Exercise training differentially modifies age-associated alteration in expression of Na$^+$-K$^+$-ATPase subunit isoforms in rat skeletal muscles. *Am. J. Physiol. Regul. Integr. Comp. Physiol.* 285:R733–R740. http://dx.doi.org/10.1152/ajpregu.00266.2003

Orlowski, J., and J.B. Lingrel. 1988. Tissue-specific and developmental regulation of rat Na,K-ATPase catalytic alpha isoform and beta subunit mRNAs. *J. Biol. Chem.* 263:10436–10442.

Radzyukevich, T.L., A.E. Moseley, D.A. Shelly, G.A. Redden, M.M. Behbehani, J.B. Lingrel, R.J. Paul, and J.A. Heiny. 2004. The Na$^+$-K$^+$-ATPase α_2-subunit isoform modulates contractility in the perinatal mouse diaphragm. *Am. J. Physiol. Cell Physiol.* 287:C1300–C1310. http://dx.doi.org/10.1152/ajpcell.00231.2004

Radzyukevich, T.L., J.B. Lingrel, and J.A. Heiny. 2009. The cardiac glycoside binding site on the Na,K-ATPase α2 isoform plays a role in the dynamic regulation of active transport in skeletal muscle. *Proc. Natl. Acad. Sci. USA.* 106:2565–2570. http://dx.doi.org/10.1073/pnas.0804150106

Radzyukevich, T.L., J.C. Neumann, T.N. Rindler, N. Oshiro, D.J. Goldhamer, J.B. Lingrel, and J.A. Heiny. 2013. Tissue-specific role of the Na,K-ATPase α2 isozyme in skeletal muscle. *J. Biol. Chem.* 288:1226–1237. http://dx.doi.org/10.1074/jbc.M112.424663

Rakowski, R.F., D.C. Gadsby, and P. De Weer. 1997. Voltage dependence of the Na/K pump. *J. Membr. Biol.* 155:105–112. http://dx.doi.org/10.1007/s002329900162

Rasmussen, M.K., M. Kristensen, and C. Juel. 2008. Exercise-induced regulation of phospholemman (FXYD1) in rat skeletal muscle: implications for Na$^+$/K$^+$-ATPase activity. *Acta Physiol. (Oxf.).* 194:67–79. http://dx.doi.org/10.1111/j.1748-1716.2008.01857.x

Sakai, R., N. Hagiwara, N. Matsuda, H. Kassanuki, and S. Hosoda. 1996. Sodium—potassium pump current in rabbit sino-atrial node cells. *J. Physiol.* 490:51–62. http://dx.doi.org/10.1113/jphysiol.1996.sp021126

Sejersted, O.M., and G. Sjøgaard. 2000. Dynamics and consequences of potassium shifts in skeletal muscle and heart during exercise. *Physiol. Rev.* 80:1411–1481.

Semb, S.O., and O.M. Sejersted. 1996. Fuzzy space and control of Na$^+$, K$^+$-pump rate in heart and skeletal muscle. *Acta Physiol. Scand.* 156:213–225. http://dx.doi.org/10.1046/j.1365-201X.1996.211000.x

Shinoda, T., H. Ogawa, F. Cornelius, and C. Toyoshima. 2009. Crystal structure of the sodium-potassium pump at 2.4 Å resolution. *Nature.* 459:446–450. http://dx.doi.org/10.1038/nature07939

Shorten, P.R., and T.K. Soboleva. 2007. Anomalous ion diffusion within skeletal muscle transverse tubule networks. *Theor. Biol. Med. Model.* 4:18. http://dx.doi.org/10.1186/1742-4682-4-18

Sweadner, K.J. 1989. Isozymes of the Na$^+$/K$^+$-ATPase. *Biochim. Biophys. Acta.* 988:185–220. http://dx.doi.org/10.1016/0304-4157(89)90019-1

Therien, A.G., and R. Blostein. 2000. Mechanisms of sodium pump regulation. *Am. J. Physiol. Cell Physiol.* 279:C541–C566.

Tokhtaeva, E., R.J. Clifford, J.H. Kaplan, G. Sachs, and O. Vagin. 2012. Subunit isoform selectivity in assembly of Na,K-ATPase α-β heterodimers. *J. Biol. Chem.* 287:26115–26125. http://dx.doi.org/10.1074/jbc.M112.370734

Vedovato, N., and D.C. Gadsby. 2014. Route, mechanism, and implications of proton import during Na$^+$/K$^+$ exchange by native Na$^+$/K$^+$-ATPase pumps. *J. Gen. Physiol.* 143:449–464. http://dx.doi.org/10.1085/jgp.201311148

Vyskočil, F., P. Hník, H. Rehfeldt, R. Vejsada, and E. Ujec. 1983. The measurement of K$_e^+$ concentration changes in human muscles during volitional contractions. *Pflugers Arch.* 399:235–237. http://dx.doi.org/10.1007/BF00656721

Wallinga, W., S.L. Meijer, M.J. Alberink, M. Vliek, E.D. Wienk, and D.L. Ypey. 1999. Modelling action potentials and membrane currents of mammalian skeletal muscle fibres in coherence with potassium concentration changes in the T-tubular system. *Eur. Biophys. J.* 28:317–329. http://dx.doi.org/10.1007/s002490050214

Williams, M.W., W.G. Resneck, T. Kaysser, J.A. Ursitti, C.S. Birkenmeier, J.E. Barker, and R.J. Bloch. 2001. Na,K-ATPase in skeletal muscle: two populations of β-spectrin control localization in the sarcolemma but not partitioning between the sarcolemma and the transverse tubules. *J. Cell Sci.* 114:751–762.

Woods, C.E., D. Novo, M. DiFranco, and J.L. Vergara. 2004. The action potential-evoked sarcoplasmic reticulum calcium release is impaired in mdx mouse muscle fibres. *J. Physiol.* 557:59–75. http://dx.doi.org/10.1113/jphysiol.2004.061291

Zhang, L., K.J. Morris, and Y.C. Ng. 2006. Fiber type-specific immunostaining of the Na$^+$,K$^+$-ATPase subunit isoforms in skeletal muscle: Age-associated differential changes. *Biochim. Biophys. Acta.* 1762:783–793. http://dx.doi.org/10.1016/j.bbadis.2006.08.006